Glycobiology vol. 18 no. 9 pp. 698–706, 2008
doi:10.1093/glycob/cwn048
Advance Access publication on May 28, 2008

Functional properties of the carboxy-terminal host cell-binding domains of the two toxins, TcdA and TcdB, expressed by *Clostridium difficile*

Tanis Dingle[2], Stefanie Wee[2], George L Mulvey[2], Antonio Greco[3], Elena N Kitova[4], Jiangxiao Sun[4], Shuangjun Lin[4], John S Klassen[4], Monica M Palcic[4], Kenneth K S Ng[3], and Glen D Armstrong[1,2]

[2]Department of Microbiology and Infectious Diseases; [3]Department of Biological Sciences, University of Calgary, Calgary, AB T2N 1N4, Canada; and [4]Department of Chemistry, University of Alberta, Edmonton, AB T6G 2R3, Canada

Received on March 20, 2008; revised on May 22, 2008; accepted on May 25, 2008

The biological and ligand-binding properties of recombinant C-terminal cell-binding domains (CBDs) and subdomains of the two large exotoxins, Toxin A (TcdA) and Toxin B (TcdB) expressed by *Clostridium difficile* were examined in the hemagglutination and Verocytotoxicity neutralization assays and by qualitative affinity chromatography using Sepharose-linked αGal(1,3)βGal(1,4)βGlc as well as the direct electrospray ionization mass spectrometry (ES-MS) assay. These studies revealed that, whereas the full-length TcdA CBD agglutinated rabbit erythrocytes, neutralized TcdA-mediated Vero cell death and bound to αGal(1,3)βGal(1,4)βGlc-derivatized Sepharose, the TcdB CBD was inactive in these functional assays. Moreover, retention by αGal(1,3)βGal(1,4)βGlc-derivatized Sepharose corresponded to the number of available TcdA subdomain ligand-binding sites. By contrast, the ES-MS assays revealed that both the TcdA and TcdB CBD bind to 8-methoxycarbonyloctyl-αGal(1,3)βGal(1,4)βGlc sequences with similar avidities. Additional ES-MS experiments using chemically altered αGal(1,3)βGal(1,4)βGlc sequences also revealed that the TcdA and TcdB CBD will tolerate a fair amount of structural variation in their complementary glycan ligands. Although the studies are consistent with the known ligand-binding properties of the TcdA and TcdB holotoxins, they also revealed subtle heretofore unrecognized functional differences in their receptor recognition properties.

Keywords: affinity/*Clostridium difficile*/ligand binding/mass spectroscopy/toxin

Introduction

Clostridium difficile is a Gram-positive, spore forming, strict anaerobe which is responsible for a suite of human pathological conditions collectively referred to as *C. difficile*-associated disease (CDAD) (Bartlett 2008). *C. difficile* infections occur frequently in hospitalized subjects who are receiving common broad spectrum antibiotic treatment because their capacity to fight infections is diminished (Owens et al. 2008). The antibiotics administered to these individuals eliminate their normal gastrointestinal (GI) microflora thereby rendering their intestines vulnerable to opportunistic colonization by *C. difficile* organisms which display an innate resistance to many conventional antimicrobial agents. Once established in the gut, *C. difficile* expresses two very large toxins, one defined as an enterotoxin, Toxin A (TcdA), and the other, a cytotoxin, Toxin B (TcdB) (Just and Gerhard 2004; Voth and Ballard 2005). It is presently believed that TcdA and TcdB are primarily responsible for the clinical signs of CDAD.

More recently, a hypervirulent strain of *C. difficile* has emerged in Europe, the USA and Canada (Blossom and McDonald 2007). This NAP1/BI/027 strain, which is fluoroquinolone resistant, is responsible for greater morbidity and mortality and possesses a mutated version of a gene, *tcdC*, whose product normally negatively controls the expression of TcdA and TcdB (McDonald et al. 2005). As a consequence of this mutation, TcdA and TcdB production in this *C. difficile* strain is unregulated and this may be responsible for its hypervirulent phenotype.

The conventional treatment for CDAD is to substitute the offending antibiotic with one, typically metronidazole, which is effective against the majority of *C. difficile* strains (Gerding et al. 2008). Vancomycin may also be used to effectively treat CDAD but only in the minority of cases where metronidazole is contraindicated. This is because of concerns its use may promote the acquisition of vancomycin resistance in organisms where this drug represents the last line of defense (Owens et al. 2008). In approximately 80% of cases, a course of metronidazole is sufficient to affect a cure and no further intervention is needed. In 20% of cases, however, CDAD may recur after treatment is finished (Maroo and LaMont 2006). For as yet uncertain reasons, some of these subjects may suffer from multiple recurring episodes of CDAD. The hypervirulent NAP1/BI/027 *C. difficile* strain also appears to be associated with a greater incidence of recurring CDAD.

The failure of the conventional mode of therapeutic intervention to prevent recurring CDAD, as well as the more recent emergence of hypervirulent strains, has prompted a renewed interest in developing alternate ways of treating *C. difficile* infections (Gerding et al. 2008). To date, most research has focused on using various probiotic organisms to prevent *C. difficile* from colonizing the GI tract. Alternate intervention strategies directed at eliminating TcdA and TcdB from the pathogenic process are also being explored. Both these strategies are directed at eliminating the use of antibiotics to treat CDAD thereby allowing the normal gut microflora to reestablish itself and resume its innate antimicrobial role in pathogen exclusion.

[1]To whom correspondence should be addressed: Tel: 1+403-220-6885; Fax: 1-403-270-2772; e-mail: glen.armstrong@ucalgary.ca

TcdA and TcdB, like other large clostridial toxins, are high molecular weight single-subunit polypeptides consisting of at least four functional domains: an amino-terminal glucosyltransferase, followed by an autocatalytic cysteine protease domain, hydrophobic membrane-spanning sequence, and highly repetitive carboxy-terminal host-cell-binding domain (CBD) (Just and Gerhard 2004; Voth and Ballard 2005; Egerer et al. 2007). Recent work has defined the three-dimensional structures of the glucosyltransferase domain and portions of the CBD, but the overall structure of the entire toxin is not well understood (Ho et al. 2005; Reinert et al. 2005; Greco et al. 2006; Aktories 2007; Jank et al. 2007). The role of the CBD is to anchor the toxins to their host cell receptors on intestinal epithelial cells which initiate the internalization process which ultimately delivers their amino-terminal enzymatic domains to the cytoplasmic compartment of the targeted cell. The enzymatic portion of TcdA and TcdB is a glucosyltransferase which covalently inactivates the Rho, Rac, and Cd42 family of proteins which control cytoskeletal function and architecture in eukaryotic cells in a GTP-dependent manner. The net effect of this glucosyltransferase activity is diarrhea and inflammation due to apoptotic cell death of the intoxicated cells and, ultimately, loss of control of intestinal epithelial barrier function.

We (Heerze et al. 1994) and others have been exploring the possibility of using host cell receptors analogs in various forms to competitively inhibit TcdA and TcdB from binding to the surface of human intestinal epithelial cells. The rationale of this approach is to provide these toxins with binding sites in the GI tract that will divert them from their normal receptors on the host cell surface and facilitate their harmless elimination from the body. By eliminating TcdA and TcdB from the pathogenic process, the need for antibiotics in treating CDAD will be reduced, thereby allowing the normal gut microflora to become reestablished. Such an approach to therapy should be particularly effective in preventing recurring CDAD.

Although several carbohydrate receptors for TcdA, including the αGal(1,3)βGal(1,4)βGlcNAc glycan sequence on rabbit erythrocytes and hamster brush border membranes (Krivan et al. 1986; Clark et al. 1987; Pothoulakis et al. 1996), as well as a range of glycans found on human cells (Tucker and Wilkins 1991; Teneberg et al. 1996), have previously been reported, the specific receptors used by TcdA and TcdB to bind to human intestinal epithelial cells remain unknown. The investigations described herein were therefore performed in order to further define the host cell-binding activities of CBDs of TcdA and TcdB with a view to advancing the discovery of therapeutic agents capable of treating CDAD in the absence of conventional antibiotics.

Results

The ligation of cell surface receptors, FAS for example, or insertional perturbation of the plasma membrane can initiate the programmed cell death (apoptosis) pathway in eukaryotic cells. However, we detected no such activity in Vero cells for the full-length CBD or subfragments of TcdA or TcdB (Figure 1 and Table I). The TcdA and TcdB holotoxins, or the full-length toxins containing the four functional domains, are cytotoxic to Vero cells and it would appear, therefore, that the Tcd CBDs do not contribute to this cytotoxicity. The TcdA holotoxin also

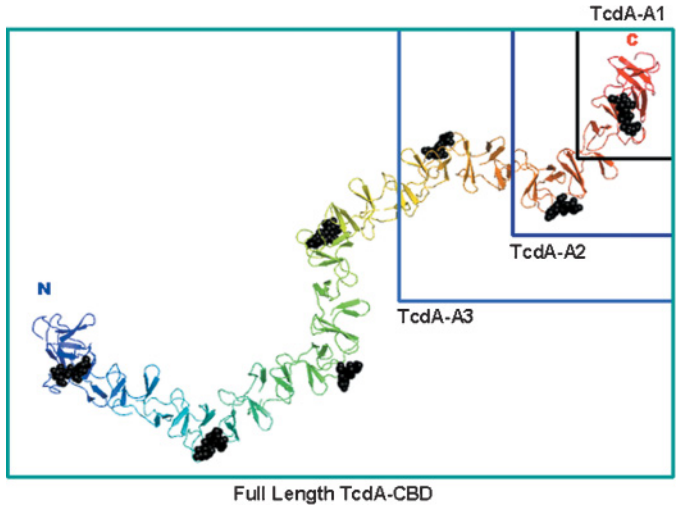

Fig. 1. Ribbon diagram of a three-dimensional model of the TcdA carboxy-terminal CBD, colored from blue to red according to sequence position (Greco et al. 2006). The binding sites for the two trisaccharide molecules seen in the TcdA-A2 crystal structure, as well as five additional sites predicted based on highly conserved sequence motifs, are denoted by space-filling representations of black trisaccharide molecules. Boxes are drawn around the carboxy-terminal subfragments TcdA-A1, TcdA-A2, and TcdA-A3, which correspond to residues 2573-2709, 2456-2710, and 2360-2710 of $TcdA_{48489}$ (numbering according to the type strain VPI 10463), respectively.

agglutinates rabbit erythrocytes. The summary data presented in Table I demonstrate that the full-length TcdA CBD, as well as its subdomains, also agglutinate rabbit erythrocytes, thereby confirming that the hemagglutinating properties of TcdA are confined to the toxin's CBD. By contrast, the full-length TcdB CBD displayed no hemagglutinating activity (Table I). The hemagglutination neutralization assay was not performed using the TcdA CBD and subfragments as they already agglutinated rabbit erythrocytes. At the highest concentration tested (8 μM), however, the full-length TcdB CBD very weakly inhibited TcdA holotoxin-mediated agglutination of rabbit erythrocytes.

Cytotoxicity neutralization assays in Vero cells were performed by competitively inhibiting TcdA or TcdB activity with the Tcd CBDs or the TcdA subfragments. Whereas the full-length TcdA CBD, as well as its A2 and A3 subfragments, competitively inhibited the cytotoxic activity of the TcdA holotoxin in Vero cells (Tables I and II), these did not inhibit the cytotoxicity of TcdB. This confirmed that the two toxins exploit different receptors on the surface of Vero cells. Although the observation that the full-length TcdB CBD failed to competitively inhibit the Verocytotoxic activity of the TcdA holotoxin is consistent with this conclusion, it also failed to competitively inhibit the cytotoxic activity of the TcdB holotoxin at the concentration tested (Table I).

The data in Figure 2 demonstrate that the hemagglutinating activity of the TcdA CBD subfragments correlated with their length, the longer peptides displaying higher hemagglutination titers than the shorter ones. Of interest, the full-length TcdA CBD more actively agglutinated rabbit erythrocytes than did the TcdA holotoxin (Figure 2).

To gain further insight into the carbohydrate-binding properties of TcdA, the A1, A2, and A3 subfragments from the C-terminus of the TcdA CBD were evaluated for binding

Table I. Summary of TcdA and TcdB CBD activities in the hemagglutination, hemagglutination neutralization, cytotoxicity, and cytotoxicity neutralization assays

	TcdA-CBD	TcdB-CBD	TcdA-A1	TcdA-A2	TcdA-A3
Hemagglutination assay	+	−	+	+	+
Cytotoxicity assay	−	−	−	−	−
Cytotoxicity neutralization of Toxin A	+	−	−	+	+
Hemagglutination neutralization	−	−[a]	−	−	−
Cytotoxicity neutralization of Toxin B	−	−	−	−	−

(+), positive result; (−), negative result.
[a]Neutralization displayed only at highest concentration (8 μM) tested.

Table II. Concentrations (IC_{50}) of the full-length TcdA-CBD and its subdomains which produced a 50% reduction in TcdA holotoxin activity in the Verocytotoxicity assay

	IC_{50} (nM)
CT_{AN} with TcdA-CBD (MW = 73, 674)	12.9
CT_{AN} with TcdA-A1 (MW = 16, 271)	None
CT_{AN} with TcdA-A2 (MW = 29, 119)	5.8
CT_{AN} with TcdA-A3 (MW = 38, 576)	3.3

Table III. Association constants (K_a, units of M^{-1}) for binding of the ligands (**1**–**5**) with TcdA-A2 and TcdB-B1 fragments, determined at 25°C and pH 7 by the direct ES-MS assay[a]

Ligand	TcdA-A2[b]	TcdB-B1
1	$5.5 \pm 0.4 \times 10^2$	$6.0 \pm 1.0 \times 10^2$
2	$6.1 \pm 1.8 \times 10^2$	$3.0 \pm 1.0 \times 10^3$
3	$4.8 \pm 2.0 \times 10^2$	$8.0 \pm 3.0 \times 10^2$
4	$8.4 \pm 1.5 \times 10^2$	$5.0 \pm 2.0 \times 10^3$
5	$9.8 \pm 2.4 \times 10^2$	$2.0 \pm 1.0 \times 10^3$

[a]Errors correspond to one standard deviation.
[b]Values are apparent-binding constants and have not been corrected for the number of binding sites.

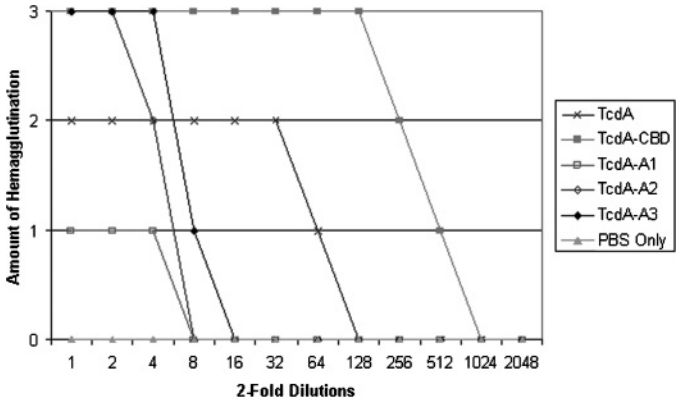

Fig. 2. Agglutination of rabbit erythrocytes in the presence of TcdA holotoxin, the full-length TcdA CBD, as well as its subdomains TcdA-A1, TcdA-A2 and, TcdA-A3. The scoring system used on the *Y*-axis is none (0), minimal (1), moderate (2), and complete hemagglutination (3).

to αGal(1,3)βGal(1,4)βGlc immobilized on Sepharose (CD-Sepharose). The A1 fragment, which only contains a single trisaccharide-binding site, bound weakly and was washed off the affinity resin after 1–2 column volumes of buffer (Figure 3). The A2 fragment containing two binding sites bound more strongly to CD-Sepharose and was only partially washed off after 5 column volumes. The A3 subfragment bound most strongly and was eluted from the affinity resin only after 20 mM **1** was added to compete for binding. Although all fragments showed some level of binding interaction with CD-Sepharose, fragments with more binding sites clearly showed a higher level of binding avidity.

Using the ES-MS assay, we evaluated the binding stoichiometry and affinity (K_a) for the CBD subfragments, TcdA-A2 and TcdB-B1, binding to the synthetic receptor **1** and receptor analogs **2**–**5** (Figure 4). Shown in Figure 5A–D are representative nanoflow ES (nanoES) mass spectra acquired for solutions of **1** with A2 or B1, at 25 and 10°C. In each case, ions corresponding to the unbound fragments, as well as fragments bound to one or two molecules of **1**, were detected (i.e., $(A2 + q\mathbf{1})^{n+}$ and $(B1 + q\mathbf{1})^{n+}$ where q = 0–3). Taken on their own, these results suggest that each of the fragments possess two binding sites for **1**. However, also detected were ions corresponding to unbound and bound P_{ref} (i.e., $(P_{ref} + q\mathbf{1})^{n+}$ where q = 0–2), which indicates that nonspecific binding of **1** to the fragments during the ES process contributed to the mass spectrum and, thereby, obscured the true binding stoichiometry in solution. Shown in Figure 6A–D are the corresponding distributions of **1** bound to A2 and B1, respectively, before and after correction for nonspecific binding. The distributions obtained at 25°C reveal that, at the concentrations investigated, both toxin fragments were bound to a maximum of one molecule of **1**. The distributions obtained at 10°C reveal the presence of a second binding site for A2, consistent with the crystal structure data, but only a single site for B1. The apparent binding constants, which were calculated from the corrected distributions for A2 and B1, are listed in Table III. At 25°C, the A2 and B1 fragments exhibit similar weak binding, with K_a values ∼500 M^{-1}. There is an increase in the affinities for both fragments at 10°C (2500 M^{-1} for A2 and 850 M^{-1} for B1) compared to 25°C, indicating that the corresponding binding enthalpies are negative. Notably, the two A2 binding sites exhibit similar affinities of 1200 M^{-1} and 1000 M^{-1} for **1**.

Affinity measurements were also performed at 25°C for A2 and B1 binding with **2**–**5**, and the apparent K_a values are listed in Table III. Notably, modification (substituting with *N*-acetyl-glucosamine, structure **2**, or a carboxylate group, structure **3**) of the glucose had a negligible effect on the K_a for A2, suggesting that the αGal(1,3)βGal disaccharide moiety may be the minimum binding epitope recognized by the toxin. In the case of B1, the *N*-acetyl-glucosamine analog **2** exhibited a five-fold increase in K_a, whereas the K_a for the disaccharide analog **3** is similar to that of **1**. Bulky substitutions to the terminal hexose

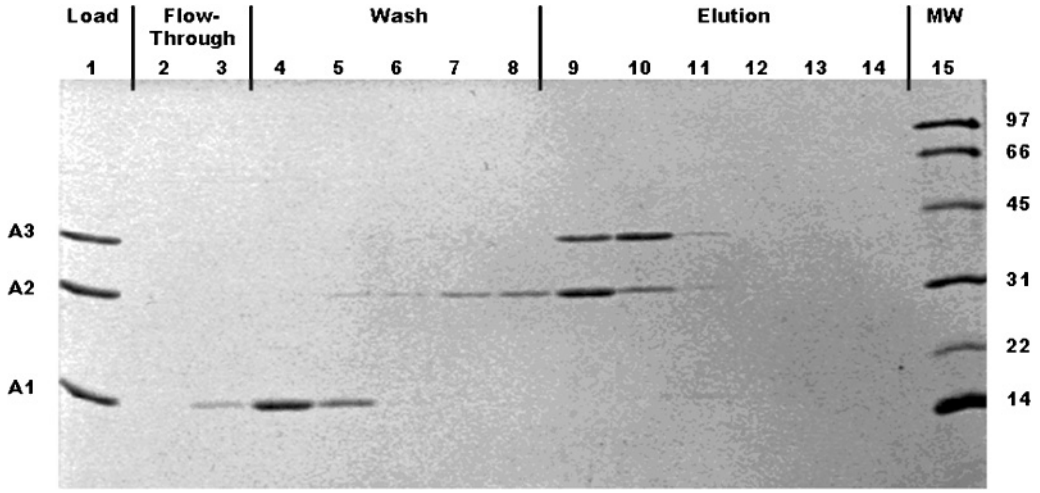

Fig. 3. Evaluation of carbohydrate-binding in TcdA-A1, -A2 and -A3 by affinity chromatography on CD-Sepharose. Each load, wash and elution fraction was 0.4 mL, the packed bed volume of the column was 0.4 mL, and the flow rate was 0.02 mL/min. Approximately 60 μg of TcdA-A1, -A2 and -A3 were loaded onto the column, and 10 μL of each fraction was analyzed by SDS–PAGE (15% acrylamide). The molecular weights (kDa) of standard proteins are indicated at the right.

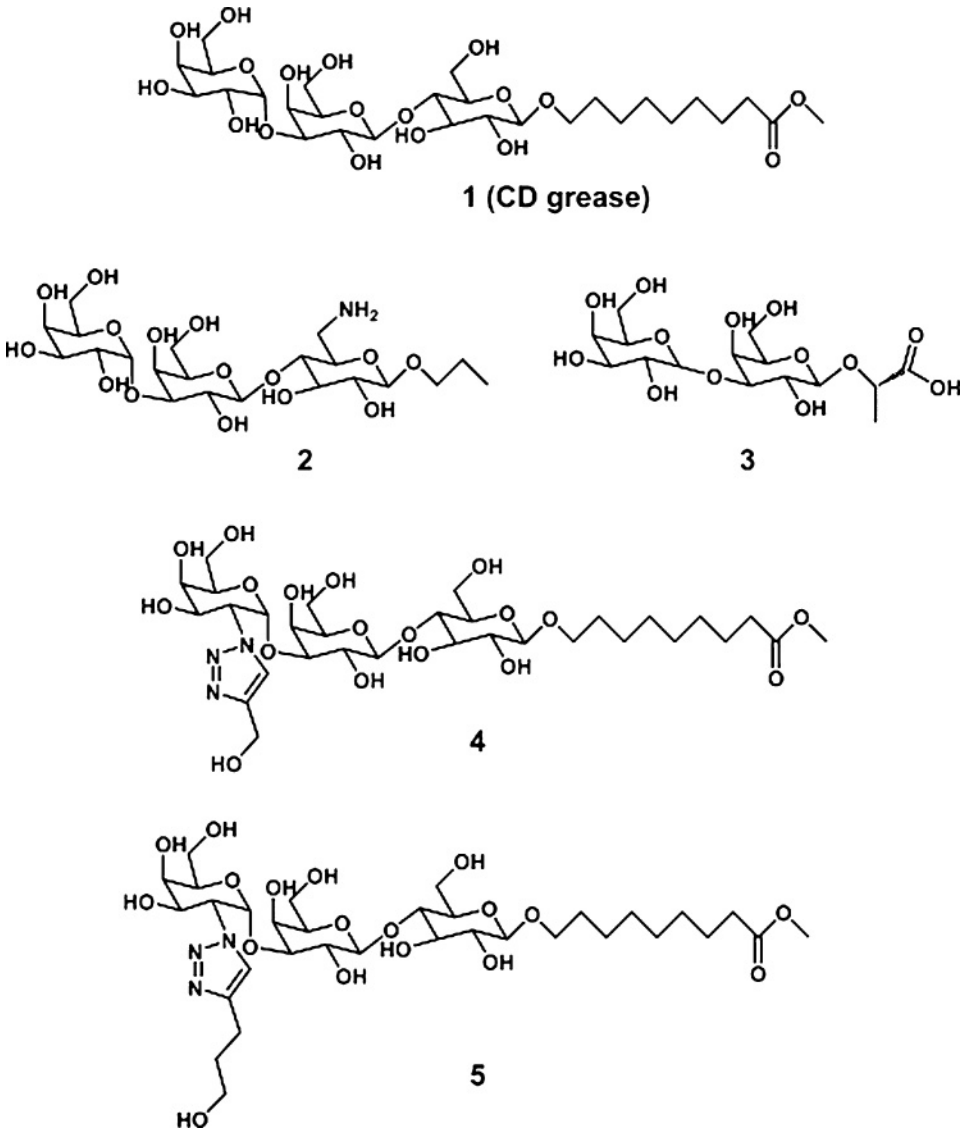

Fig. 4. Ligand structures.

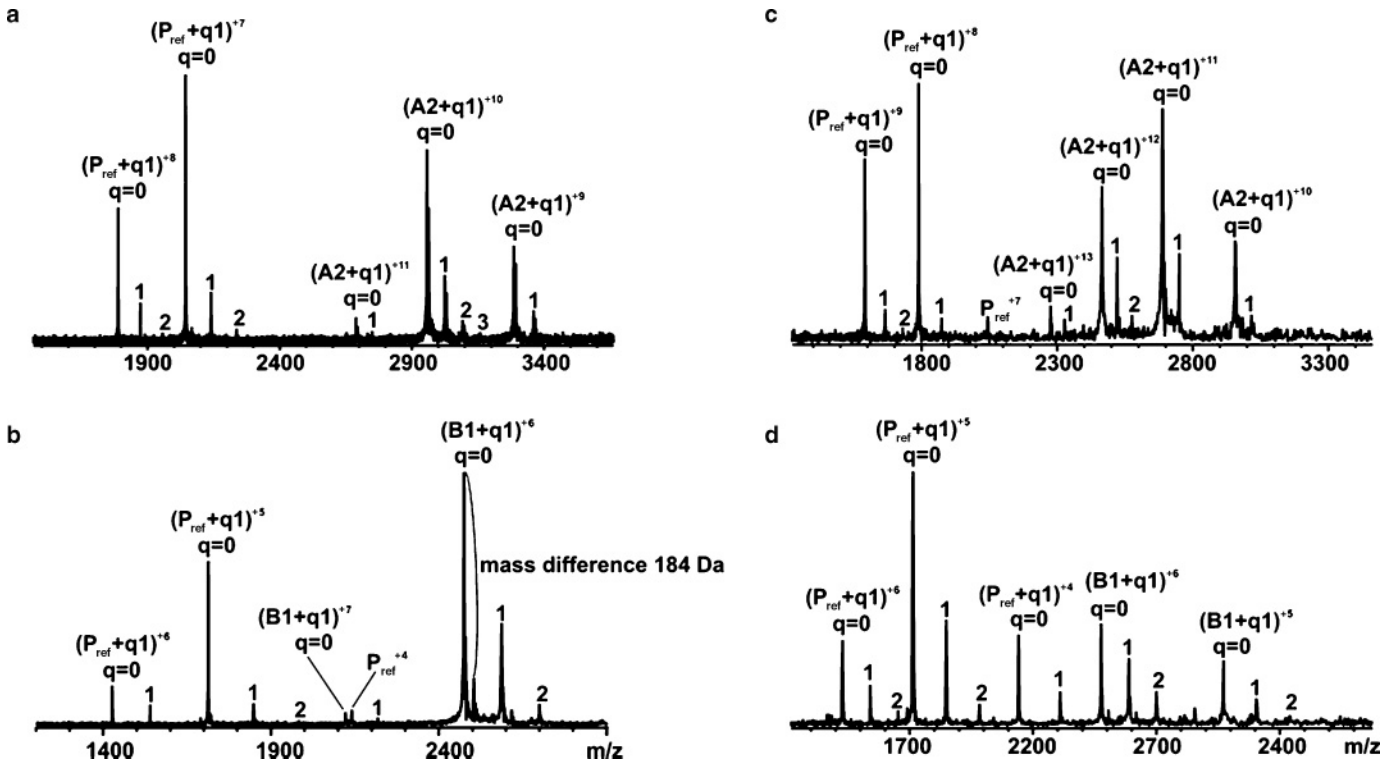

Fig. 5. NanoES mass spectra of solutions consisting of (**A**) 14 μM A2 and 150 μM **1** at pH 7 and 25°C, (**B**) 5 μM B1 and 35 μM **1** at pH 7 and 25°C (**C**) 14 μM A2 and 110 μM **1** at pH 7 and 10°C, (**D**) 14 μM B1 and 120 μM **1** at pH 7 and 10°C. A reference protein (P_{ref}) was added to each solution to quantify the extent of nonspecific protein-ligand binding during the ES process.

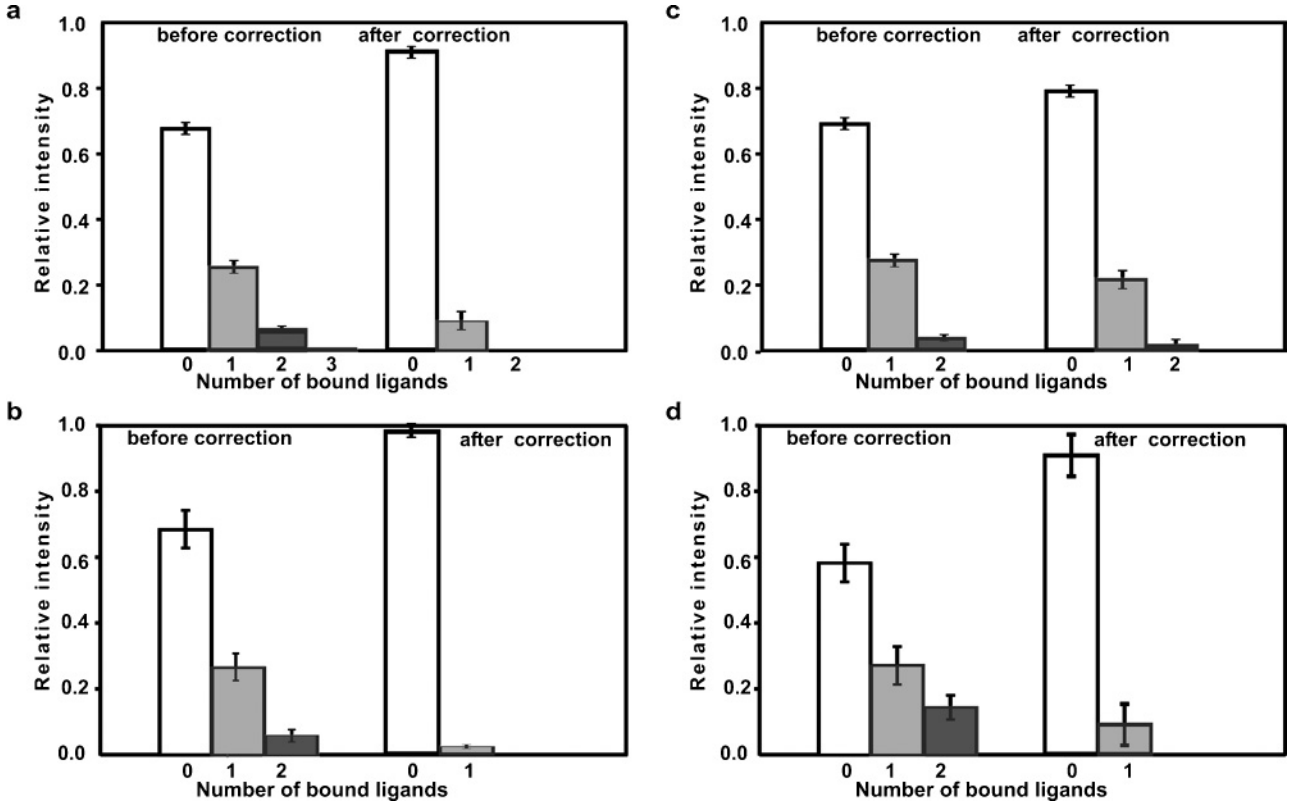

Fig. 6. Distributions of **1** bound to A2 (**A**, **C**) and B1 (**B**, **D**) before and after correction for nonspecific ligand binding, as determined from the mass spectra shown in Figure 5.

lead to a moderate (two-fold) increase in the K_a values for A2, but a more substantial, three- to eight-fold increase for B1.

Discussion

Although TcdA binds to αGal(1,3)βGal(1,4)βGlc glycan sequences on rabbit erythrocytes (Krivan et al. 1986), this receptor is not present on human intestinal epithelial cells (Tucker and Wilkins 1991). However, TcdA also binds to Lewis X, Y, and I glycan sequences which are expressed on the surface of human intestinal epithelial cells (Tucker and Wilkins 1991; Smith et al. 1997). These findings, in addition to the ES-MS data presented in Table III, indicate that TcdA is a promiscuous glycan-binding protein which can tolerate a significant amount of structural variation in the carbohydrate sequences it is capable of ligating on host cell surfaces. In a further attempt to identify TcdA and TcdB receptors on human epithelial cells, the TcdA-A2 and TcdB-B1 subfragments were recently screened at the Consortium for Functional Glycomics (CFG, www.functionalglycomics.org) glycan micro-array facility. This micro-array contains over 350 unique complex carbohydrate sequences. The results, which can be accessed at http://www. functionalglycomics.org/ glycomics/ publicdata/selectedScreens.jsp from December 6, 2007, show that Le^a-LacNAc and Sia-Le^a-Le^x may also be potential receptor candidates for the TcdA-A2 subfragment. In contrast, the micro-array screen revealed no obvious receptor glycan sequences for the TcdB-B1 subfragment (http://www.functionalglycomics.org/glycomics/publicdata/selectedScreens.jsp from December 6, 2007). This observation suggests that, if like TcdA, TcdB also binds to a glycan receptor sequence on host cells; this receptor is not yet represented on the CFG micro-array. However, given the promiscuous behavior of TcdA, it would seem unlikely that TcdB would fail to bind any obvious glycans on the micro-array suggesting that this toxin may bind to host cell surfaces by a novel mechanism which may not involve complex carbohydrate sequences. This interpretation is also consistent with the differences in the functional properties (Table I) we observed for the TcdA and TcdB CBDs.

The TcdA and TcdB CBDs consist of blocks of repeating sequence containing 21, 30, or 50 amino acids (Dove et al. 1990; Eichel-Streiber and Sauerborn 1990; Ho et al. 2005). Crystal structures of TcdA fragments indicate that these repeating sequence motifs form 32 short repeats (SRs) and 7 long repeats (LRs) in the TcdA CBD that combine to form seven carbohydrate-binding sites (Ho et al. 2005; Greco et al. 2006). In TcdB, a similar series of repeating sequence motifs are predicted to form 19 SRs and 4 LRs that may also form four carbohydrate-binding sites. Like many carbohydrate-binding proteins, the affinity of a single binding site for its complementary glycan ligand is typically very low. We confirmed this principle for the TcdA and TcdB CBD's binding to its rabbit erythrocyte glycan receptor **1** using a qualitative affinity chromatography approach, as well as the ES-MS technique, which is exquisitely sensitive as well as responsive to low affinity interactions.

Nature, however, compensates for low affinity protein-glycan-binding interactions by multiplying the number of available binding sites thereby increasing the avidity of the binding process. This is typically achieved by allowing carbohydrate-binding proteins containing only one glycan-binding domain to assemble into multi-subunit complexes. The Shiga toxin B subunit for example or, as recently revealed by the TcdA CBD X-ray crystal structure, express multiple repeating glycan-binding domains in a single extended polypeptide (Kitov et al. 2000; Greco et al. 2006). The findings that the shorter TcdA CBD fragments produced lower titers in the hemagglutination assay (Figure 2) and are less retarded by interactions in affinity chromatography (Figure 3) are also consistent with this general principle. Fragments possessing fewer glycan-binding sites appear to have a lower avidity for the surface of rabbit erythrocytes and for binding sites in the affinity chromatography column.

The ES-MS experiments also revealed that the glycan-binding domains of TcdA and TcdB will tolerate a fair amount of structural variation in their complementary glycan ligands. This finding is consistent with the open trisaccharide-binding site seen in the crystal structure for TcdA-A2 bound to αGal(1,3)βGal(1,4)βGlcNAc (12). This could explain the finding that, whereas TcdA binds to the αGal(1,3)βGal(1,4)βGlcNAc sequence on rabbit erythrocytes, a different carbohydrate structure must be recognized in human intestinal epithelial cells, since the αGal(1,3)Gal linkage is not found in humans (Macher and Galili 2008). Given their apparent central role in the pathogenic process, TcdA's tolerance for structural variability in its glycan receptors may also explain why *C. difficile* causes opportunistic infections in a number of mammalian species besides humans.

One of the most striking findings from the current study is that the C-terminal carbohydrate-binding repeat in TcdB shows comparable binding affinity for αGal(1,3)βGal(1,4)βGlc when compared with individual CBD repeats from TcdA, even though hemagglutination and cytotoxicity neutralization assays indicate a dramatic difference in cell-surface receptor binding. Differences in the cell-surface receptor-binding specificities of TcdA and TcdB have been reported in several previous studies and are consistent with the hemagglutination and cytotoxicity studies reported here (Krivan et al. 1986; Chaves-Olarte et al. 1997).

Further work is clearly required to provide a molecular structural basis for understanding why single binding sites of TcdA and TcdB can recognize similar monomeric ligands, but full-length toxins show very different receptor-binding specificities. A possible explanation is that the three-dimensional arrangement of individual carbohydrate-binding sites in TcdB may differ significantly from that of TcdA. As a result, the cell-surface receptors found on rabbit erythrocytes and Vero cells that are bound with high avidity by TcdA may be arranged in a manner that is incompatible with the arrangement of carbohydrate-binding sites in TcdB. In support of this hypothesis, differences in the spacing of LRs are clearly seen in the sequences of CBDs from TcdA and TcdB (Ho et al. 2005; Greco et al. 2006). Unfortunately, the effects of these differences on the three-dimensional arrangement of carbohydrate-binding sites are not known at present. Further work to define the nature and arrangement of carbohydrate-binding repeats in both TcdA and TcdB, as well as the nature of cell-surface receptors, is clearly needed to test this hypothesis.

A second possible explanation for the difference in cell-surface receptor-binding specificity is that a second domain in TcdB, apart from the C-terminal CBD, may be important for cell-surface binding. Our observation that high concentrations (8 μM) of the TcdB CBD failed to inhibit the cytotoxicity of TcdB is consistent with this hypothesis. Because the deletion of the C-terminal CBD of TcdB decreases cytotoxicity by 10-fold,

it seems likely that the CBD plays an important role in cell-surface receptor binding, but other parts of the protein may also be involved (Barroso et al. 1994). Further work is clearly needed to test this hypothesis as well.

Materials and methods

Proteins

The TcdA and TcdB holotoxins were purified from *C. difficile* VPI 10463 (ATCC 43255) as described previously (Heerze et al. 1994). The full-length CBD of TcdA from *C. difficile* strain 48489 (toxinotype VI), as well as the TcdA-A1 and A2 subfragments (previously referred to as TcdA-f1 and TcdA-f2) (Figure 1), was cloned, expressed in *Escherichia coli,* and purified as described previously (Ho et al. 2005; Greco et al. 2006). The pET-3a expression clone for TcdA-A3 was generated in a similar manner using PCR (forward primer = 5′ G GAA TTC CAT ATG CAC CAT CAC CAT CAC CAT AAT ACT AAC ATT GCT GAA GTA GCT ACT and reverse primer as for TcdA-A2) to amplify the region of $TcdA_{48489}$ corresponding to amino acids 2360-2710 of $TcdA_{10463}$. The full-length CBD of TcdB from *C. difficile* strain VPI 10463 (toxinotype 0) was cloned, expressed in *E. coli* with an N-terminal glutathione-*S*-transferase fusion protein, purified by standard methods using affinity chromatography with glutathione-Sepharose (GE Healthcare, Piscataway, NJ) according to instructions from the manufacturer, and eluted from the column by cleavage with thrombin. The pET-3a expression clone for TcdB-B1 was generated using PCR (forward primer = 5′-G GAA TTC CAT ATG CAC CAT CAC CAT CAC CAT AAG GGC ATA ATG AGA ACG GGT CTT ATA TC-3′ and reverse primer = 5′-CG GGA TCC TTA TTC ACT AAT CAC TAA TTG AGC-3′). Lysozyme and ubiquitin, which served as reference proteins (P_{ref}) for the ES-MS binding assays, were purchased from Sigma–Aldrich (Oakville, ON), and used without further purification.

Synthetic ligands

The trisaccharide αGal(1,3)βGal(1,4)GlcO$(CH_2)_8CO_2CH_3$ (CD-grease), **1**, was prepared as described previously (Ratcliffe et al. 2004). The structurally related trisaccharides, αGal(1–3)βGal(1–4)βGlc[6-NH_2]-O-$(CH_2)_2CH_3$, **2**, the hydroxymethyltriazole derivative of αGal(1–3)βGal(1–4)βGlcO-C8-$COOCH_3$, **4**, and the hydroxypropyltriazole derivative of αGal(1–3)βGal(1–4)βGlcO-C8-$COOCH_3$, **5**, as well as the disaccharide αGal(1–3)βGal-O-[2-(S)-propionic acid], **3**, were kindly provided by Dr David R. Bundle (University of Alberta). The structures of the di- and trisaccharides are shown in Figure 4.

Synthesis of CD-Sepharose

1 was converted to its ethylenediamine monoamide by reaction with neat anhydrous ethylenediamine (Zhang et al. 1995) and then coupled to cyanogen bromide-activated Sepharose 4B to form CD-Sepharose. The incorporation level was 12 μmol **1** per mL of resin.

Affinity chromatography

A column (4.6 mm diameter × 30 mm) packed with 0.4 mL of CD-Sepharose was equilibrated in a loading buffer (50 mM Tris–HCl, pH 8.0, 300 mM NaCl, 5% (w/v) glycerol). A mixture (0.4 mL) of A1, A2, and A3, each present at a concentration of 0.15 mg/mL and dialyzed against the loading buffer, was loaded onto the column, washed with 2 mL of loading buffer and then eluted with 2 mL of 15 mg/mL αGal(1,3)βGal(1,4)GlcO$(CH_2)_8CO_2CH_3$ dissolved in the loading buffer. Fractions (0.4 mL) were collected, and a 10 μL sample of each fraction was analyzed by sodium dodecylsulfate–polyacrylamide gel electrophoresis (SDS–PAGE) (15% acrylamide).

Hemagglutination assay

The TcdA CBDs were serially diluted, beginning at an equimolar concentration of 8 μM each in sodium/potassium phosphate-buffered (pH 7.2) physiological saline (PBS) in Costar brand 96 round-bottom well plates. A 4% (v/v) solution of freshly prepared rabbit erythrocytes in PBS was then added 1:1 with gentle mixing to each of the wells and the plates were incubated overnight at 4°C before visually scoring them for hemagglutination.

Cytotoxicity assay

The cytotoxicity assay involved preparing serial dilutions of the full-length CBD or subdomains of TcdA and TcdB in minimal essential medium (MEM) in 96-well tissue culture plates. The starting concentration for each dilution series was 0.11 mg/mL for the full-length TcdA CBD, 0.24 mg/mL for TcdA-A1, 0.09 mg/mL for TcdA-A2, 0.10 mg/mL for TcdA-A3, and 0.06 mg/mL for the full-length TcdB CBD. From each of these wells 20 μL was then transferred to a 96-well tissue culture plate containing confluent monolayers of African green monkey kidney (Vero) cells. The plates were incubated overnight at 37°C in an atmosphere containing 5% CO_2. 3-4,5-Dimethylthiazoyl-2-2,5 diphenyltetrazolium bromide (MTT, Sigma-Aldrich) was then added to a final concentration of 0.5 mg/mL to each of the wells. The plates were incubated for an additional 4 h at 37°C before replacing their contents with 200 μL of 5 mM HCl containing 5% (w/v) sodium dodecylsulfate. After 18 h of further incubation at 37°C, the results were recorded using a Spectramax model 340 microtiter plate reader (Molecular Devices, Sunnyvale, CA) set to a wavelength of 570 nm.

Cytotoxicity neutralization assay

The CBD and subdomains of TcdA and TcdB were serial diluted, starting from a concentration of 0.82 μM, in PBS in 96-well microtiter plates. Twenty microliter of each dilution was then admixed with the TcdA or TcdB holotoxins, each diluted in 180 μL of PBS to their CD_{100} concentration (minimum concentration resulting in a 100% cytopathic effect) in the Vero-cytotoxicity assay. From each of these wells 20 μL was then transferred to a 96-well microtiter plate containing confluent Vero cell monolayers in MEM. The plates were incubated for 4 h at 37°C before the medium in each well was removed and replaced with fresh MEM supplemented with 10% fetal bovine serum (FBS). The plates were incubated for an additional 24 h and cell viability was assessed using MTT as described in the previous section.

Electrospray ionization mass spectrometry-binding assays

Association constants (K_a) for the fragments TcdA-A2 and TcdB-B1 binding to the synthetic trisaccharide receptor **1** and receptor analogs **2–5** were evaluated using the direct electrospray ionization mass spectrometry (ES-MS) assay. Complete details of the experimental methodology and data analysis have been described elsewhere (Wang et al. 2003, 2005; Sun et al. 2006) and only a brief overview is given here. The ES-MS measurements were carried out using a 9.4 T ApexII Fourier-transform ion cyclotron resonance (FT-ICR) MS (Bruker-Daltonics, Billerica, MA) equipped with a temperature-controlled nanoflow ES device (Daneshfar et al. 2004). Prior to analysis, the TcdA-A2 and TcdB-B1 solutions were dialyzed against 50 mM ammonium acetate (pH 7.2) using Amicon Ultra-4 centrifugal filters (Millipore, Billerica, MA) with a molecular weight cutoff of 10,000 Da. The protein concentrations of the resulting TcdA-A2 and TcdB-B1 solutions were measured by UV absorption. Each ES solution was prepared from stock solutions of protein (TcdA-A2 and TcdB-B1) and carbohydrate ligands **1–5**. Lysozyme and ubiquitin were used as controls to distinguish specific from nonspecific ligand interactions with TcdA-A2 and TcdB-B1, respectively, in the ES-MS assay. Standard deviations were calculated based on the results of five separate measurements.

Funding

Alberta Ingenuity Centre for Carbohydrate Science.

Acknowledgements

We thank Dmitry Solomon, Pavel Kitov and David Bundle for generously providing compounds **2–5**. Additionally, we gratefully acknowledge the assistance of Maja Rupnik for generously providing expression clones and for advice throughout the course of this work.

Conflict of interest statement

There are no conflicts of interest.

Abbreviations

CBD, cell-binding domain; ES-MS, direct electrospray ionization mass spectrometry; GI, gastrointestinal; LR, long repeat; MEM, minimal essential medium; MTT, 3-4,5-Dimethylthiazoyl-2-2,5-diphenyltetrazolium bromide; SDS–PAGE, sodium dodecylsulfate–polyacrylamide gel electrophoresis; SR, short repeat; TcdA, Toxin A; TcdB, Toxin B.

References

Aktories K. 2007. Self-cutting to kill: New insights into the processing of *Clostridium difficile* toxins. *ACS Chem Biol*. 2:228–230.

Barroso LA, Moncrief JS, Lyerly DM, Wilkins TD. 1994. Mutagenesis of the *Clostridium difficile* toxin B gene and effect on cytotoxic activity. *Microb Pathog*. 16:297–303.

Bartlett JG. 2008. Historical perspectives on studies of *Clostridium difficile* and *C. difficile* infection. *Clin Infect Dis*. 46(Suppl 1):S4–S11.

Blossom DB, McDonald LC. 2007. The challenges posed by reemerging *Clostridium difficile* infection. *Clin Infect Dis*. 45:222–227.

Chaves-Olarte E, Weidmann M, Eichel-Streiber C, Thelestam M. 1997. Toxins A and B from *Clostridium difficile* differ with respect to enzymatic potencies, cellular substrate specificities, and surface binding to cultured cells. *J Clin Invest*. 100:1734–1741.

Clark GF, Krivan HC, Wilkins TD, Smith DF. 1987. Toxin A from *Clostridium difficile* binds to rabbit erythrocyte glycolipids with terminal Gal alpha 1-3Gal beta 1-4GlcNAc sequences. *Arch Biochem Biophys*. 257:217–229.

Daneshfar R, Kitova EN, Klassen JS. 2004. Determination of protein-ligand association thermochemistry using variable-temperature nanoelectrospray mass spectrometry. *J Am Chem Soc*. 126:4786–4787.

Dove CH, Wang SZ, Price SB, Phelps CJ, Lyerly DM, Wilkins TD, Johnson JL. 1990. Molecular characterization of the *Clostridium difficile* toxin A gene. *Infect Immun*. 58:480–488.

Egerer M, Giesemann T, Jank T, Satchell KJ, Aktories K. 2007. Auto-catalytic cleavage of *Clostridium difficile* toxins A and B depends on cysteine protease activity. *J Biol Chem*. 282:25314–25321.

Eichel-Streiber C, Sauerborn M. 1990. *Clostridium difficile* toxin A carries a C-terminal repetitive structure homologous to the carbohydrate binding region of streptococcal glycosyltransferases. *Gene*. 96:107–113.

Gerding DN, Muto CA, Owens RC Jr. 2008. Treatment of *Clostridium difficile* infection. *Clin Infect Dis*. 46(Suppl 1):S32–S42.

Greco A, Ho JG, Lin SJ, Palcic MM, Rupnik M, Ng KK. 2006. Carbohydrate recognition by *Clostridium difficile* toxin A. *Nat Struct Mol Biol*. 13:460–461.

Heerze LD, Kelm MA, Talbot JA, Armstrong GD. 1994. Oligosaccharide sequences attached to an inert support (SYNSORB) as potential therapy for antibiotic-associated diarrhea and pseudomembranous colitis. *J Infect Dis*. 169:1291–1296.

Ho JG, Greco A, Rupnik M, Ng KK. 2005. Crystal structure of receptor-binding C-terminal repeats from *Clostridium difficile* toxin A. *Proc Natl Acad Sci USA*. 102:18373–18378.

Jank T, Giesemann T, Aktories K. 2007. Rho-glucosylating *Clostridium difficile* toxins A and B: New insights into structure and function. *Glycobiology*. 17:15R–22R.

Just I, Gerhard R. 2004. Large clostridial cytotoxins. *Rev Physiol Biochem Pharmacol*. 152:23–47.

Kitov PI, Sadowska JM, Mulvey G, Armstrong GD, Ling H, Pannu NS, Read RJ, Bundle DR. 2000. Shiga-like toxins are neutralized by tailored multivalent carbohydrate ligands. *Nature*. 403:669–672.

Krivan HC, Clark GF, Smith DF, Wilkins TD. 1986. Cell surface binding site for *Clostridium difficile* enterotoxin: Evidence for a glycoconjugate containing the sequence Gal alpha 1-3Gal beta 1-4GlcNAc. *Infect Immun*. 53:573–581.

Macher BA, Galili U. 2008. The Galalpha1,3Galbeta1,4GlcNAc-R (alpha-Gal) epitope: A carbohydrate of unique evolution and clinical relevance. *Biochim Biophys Acta*. 1780:75–88.

Maroo S, LaMont JT. 2006. Recurrent *Clostridium difficile*. *Gastroenterology*. 130:1311–1316.

McDonald LC, Killgore GE, Thompson A, Owens RC Jr, Kazakova SV, Sambol SP, Johnson S, Gerding DN. 2005. An epidemic, toxin gene-variant strain of *Clostridium difficile*. *N Engl J Med*. 353:2433–2441.

Owens RC Jr, Donskey CJ, Gaynes RP, Loo VG, Muto CA. 2008. Antimicrobial-associated risk factors for *Clostridium difficile* infection. *Clin Infect Dis*. 46(Suppl 1):S19–S31.

Pothoulakis C, Gilbert RJ, Cladaras C, Castagliuolo I, Semenza G, Hitti Y, Montcrief JS, Linevsky J, Kelly CP, Nikulasson S, et al. 1996. Rabbit sucrase-isomaltase contains a functional intestinal receptor for *Clostridium difficile* toxin A. *J Clin Invest*. 98:641–649.

Ratcliffe RM, Kamath VP, Yeske RE, Gregson JM, Fang YR, Palcic MM. 2004. Large-scale chemical and enzymatic synthesis of a *Clostridium difficile* toxin a binding trisaccharide. *Synthesis-Stuttgart*. 2293–2296.

Reinert DJ, Jank T, Aktories K, Schulz GE. 2005. Structural basis for the function of *Clostridium difficile* toxin B. *J Mol Biol*. 351:973–981.

Smith JA, Cooke DL, Hyde S, Borriello SP, Long RG. 1997. *Clostridium difficile* toxin A binding to human intestinal epithelial cells. *J Med Microbiol*. 46:953–958.

Sun J, Kitova EN, Wang W, Klassen JS. 2006. Method for distinguishing specific from nonspecific protein-ligand complexes in nanoelectrospray ionization mass spectrometry. *Anal Chem*. 78:3010–3018.

Teneberg S, Lonnroth I, Torres Lopez JF, Galili U, Halvarsson MO, Angstrom J, Karlsson KA. 1996. Molecular mimicry in the recognition of glycosphingolipids by Gal alpha 3 Gal beta 4 GlcNAc beta-binding *Clostridium*

difficile toxin A, human natural anti alpha-galactosyl IgG and the monoclonal antibody Gal-13: Characterization of a binding-active human glycosphingolipid, non-identical with the animal receptor. *Glycobiology*. 6:599–609.

Tucker KD, Wilkins TD. 1991. Toxin A of *Clostridium difficile* binds to the human carbohydrate antigens I, X, and Y. *Infect Immun*. 59:73–78.

Voth DE, Ballard JD. 2005. *Clostridium difficile* toxins: Mechanism of action and role in disease. *Clin Microbiol Rev*. 18:247–263.

Wang W, Kitova EN, Klassen JS. 2003. Influence of solution and gas phase processes on protein-carbohydrate binding affinities determined by nanoelectrospray Fourier transform ion cyclotron resonance mass spectrometry. *Anal Chem*. 75:4945–4955.

Wang W, Kitova EN, Klassen JS. 2005. Nonspecific protein-carbohydrate complexes produced by nanoelectrospray ionization. Factors influencing their formation and stability. *Anal Chem*. 77:3060–3071.

Zhang Y, Le X, Dovichi NJ, Compston CA, Palcic MM, Diedrich P, Hindsgaul O. 1995. Monitoring biosynthetic transformations of *N*-acetyllactosamine using fluorescently labeled oligosaccharides and capillary electrophoretic separation. *Anal Biochem*. 227:368–376.